THE JOURNAL OF PHYSICAL CHEMISTRY B

Article

pubs.acs.org/JPCB

Electron Transfer Dissociation Mass Spectrometry of Peptides Containing Free Cysteine Using Group XII Metals as a Charge Carrier

Daiki Asakawa*,† and Yoshinao Wada

Department of Molecular Medicine, Osaka Medical Center and Research Institute for Maternal and Child Health, 840 Murodo-cho, Izumi, Osaka 594-1101, Japan

ABSTRACT: Electron transfer dissociation (ETD) has been used for peptide sequencing. Since ETD preferentially produces the $c'/z^{\bullet}$ fragment pair, peptide sequencing is generally performed by interpretation of mass differences between series of consecutive c' and $z^{\bullet}$ ions. However, the presence of free cysteine residues in a precursor promotes peptide bond cleavage, hindering interpretation of the ETD spectrum. In the present study, the divalent group XII metals, such as Zn^{2+}, Cd^{2+} and Hg^{2+}, were used as charge carriers to produce metal-peptide complexes. The thiol group is deprotonated by complexation with the group XII metal. The formation of b and y' ions was successfully suppressed by using the zinc-peptide complex as a precursor, indicating Zn^{2+}-aided ETD to be a useful method for sequencing of cysteine-containing peptides. By contrast, ETD of Cd^{2+}– and Hg^{2+}–peptide complexes mainly led to SH_2 loss and radical cation formation, respectively. These processes were mediated by recombination energy between the metal cation and an electron. The presence of monovalent cadmium and neutral mercury in ETD products was confirmed by MS^3 analysis with collision-induced dissociation.

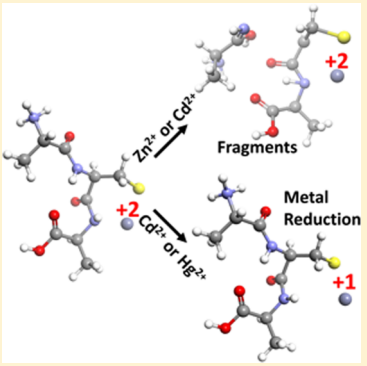

INTRODUCTION

Tandem mass spectrometry with electron-mediated fragmentation techniques, such as electron capture dissociation (ECD)[1] and electron transfer dissociation (ETD),[2] has been used for characterization of peptides. The ECD/ETD process is initiated by an electron attachment/transfer to multiply protonated molecules formed by electrospray ionization (ESI), and generates a radical reactive species which gives rise to a complementary pair of consisting a c' fragment and a $z^{\bullet}$ radical by N–C_{α} bond cleavage.[3] Since ECD/ETD involved the recombination between peptide ion and electron/anion, employing ions with a higher charge state as the precursor dramatically increases the yield of radical reactive species and thereby improving the sequence coverage obtained with ECD/ETD.[4,5] The charge state of peptides is dependent on the peptide sequence, especially on the number of basic residues. For ESI of tryptic peptides, the N-terminal amino group and the C-terminal basic residue are protonated, often yielding doubly protonated species. However, double protonation is not enough for the ion/electron reaction of ECD/ETD to yield better sequence coverage. Therefore, increasing the charge state of precursor ions is desired. The fixed charge derivatization of thiol[6,7] or a carboxyl group[8,9] has been demonstrated to increase the charge state of peptides, improving the quality of the mass spectrum. Alternatively, we reported that the complexation of peptides with metal ions increases the charge state of peptides containing acidic residues, and renders ETD spectra more informative than those obtained from protonated molecules with lower charge states.[10] With fundamental or analytical research aims, various metal cations such as alkali metals,[11] alkali-earth metals,[12,13] transmission metals,[13,14] group XII metals[13,15] and lanthanides[16] have been used for ECD/ETD experiments. In many cases, ECD/ETD of metal–peptide complexes leads to N–C_{α} bond cleavage, as well as protonated precursor. Therefore, the proposed mechanisms for N–C_{α} bond cleavage through aminoketyl radical intermediate in ECD/ETD of protonated precursor can be envisaged for a metal–peptide complex. Notably, while the N–C_{α} bond cleavage preferentially generates the c' and $z^{\bullet}$ fragment pair, ECD/ETD of metal–peptide complexes generates abundant signal of the $c^{\bullet}$ and z' fragments, which are the products of interfragment hydrogen migration between c' and $z^{\bullet}$ fragments.[10,12] The source of hydrogen in this process was investigated to be an α-carbon of the c' fragment.[17] The hydrogen migration is an exothermic reaction, and therefore high abundance of $c^{\bullet}$ and z' fragments is generally rationalized on the basis of the long c'–$z^{\bullet}$ complex lifetime to allow intramolecular hydrogen migration. Since metal cations were coordinated with several amino acid residues to form metal-peptide complexes,[18] the presence of a metal cation in the precursor for ETD increased the lifetime of the c'-$z^{\bullet}$ fragment complex, eventually generating $c^{\bullet}$ and z' fragments through interfragment hydrogen migration.[10] The degree of hydrogen migration was dependent on the location of the metal cation in the metal–peptide complex. ETD induces conformational rearrangement to give a charge-reduced form, and therefore the hydrogen migration observed in ETD mass spectrum of metal–peptide complexes represented the lowest energy conformation of their "proton-removed" precursor.[10] The interfragment hydrogen migration during ECD/ETD would

Received: March 21, 2014
Revised: September 30, 2014
Published: October 1, 2014

dx.doi.org/10.1021/jp502818u | J. Phys. Chem. B 2014, 118, 12318–12325

provide insight into the conformation of metal−peptide complexes in the gas phase.

In contrast to N−C_α bond cleavage, the recombination between a metal cation and an electron can alternatively occur in ECD/ETD of a metal−peptide complex. The aminoketyl radical formation and metal reduction in ECD/ETD can be regarded as two competing reactions. The metal reduction is promoted with increasing of reduction potential of metal cation in aqueous solution[16] such that the choice of metal has a critical effect on ECD/ETD processes. The Cu^{2+} and Eu^{3+} in the complexes are reduced by ECD/ETD and the recombination energy is redistributed throughout the peptide to give b/y' ions or neutral loss.[13,14,16] The use of group XII metal cations, Cd^{2+} and Hg^{2+} for ECD provides peptide radical cation, $M^{+\bullet}$ and related fragments by neutral metal loss from metal-peptide complex.[15] Peptide radical ions presumably formed due to reduction of divalent metal cation by ECD with an subsequent electron transfer from peptide to monovalent metal cation.[15]

The group XII metal cations, such as Zn^{2+}, Cd^{2+} and Hg^{2+}, strongly bind to the thiol group of cysteine residues in peptides or proteins. In the present study, we employed these ions as a charge carrier to increase the charge-state of peptides containing a free cysteine residue(s) and detail of the ETD processes is investigated by multistage tandem mass spectrometry. The zinc-peptide complex preferentially produced a $c'/z^\bullet$ fragment pair from cysteine-containing peptides, facilitating interpretation of the product ion mass spectrum. On the other hand, competitive reduction between a metal cation and a proton occurred in the ETD of the cadmium-peptide complex. The mercury-peptide complex produced a peptide radical cation with subsequent radical-induced cleavage by ETD.

EXPERIMENTAL SECTION

Materials and Preparation. Somatostatin and [Arg^8]-vasopressin were purchased from Peptide Institute, Inc. (Osaka, Japan). A synthetic peptide designed to mimic human serum albumin, designated HSA31−39 (LQQCPFEDH), was purchased from Sigma-Aldrich (St. Louise, MO, USA). The sequences of tested peptides are shown in Table 1. Zinc chloride ($ZnCl_2$), cadmium acetate dihydrates ($Cd(CH_3COO)_2\bullet 2H_2O$) and mercury chloride ($HgCl_2$) were purchased from Wako Pure Chemical (Osaka, Japan). All reagents were used without further purification. All of the solvents used were HPLC grade quality, except for water, which was purified employing a Milli-Q purification system (Millipore; Billerica, MA, USA).

Table 1. Monoisotopic Mass (M_m), Sequence and Composition of Analyte Peptides Containing Free Cysteine Residues Used

analyte peptide	M_m	sequence	composition
[Arg^8]-vasopressin	1085.45	CYFQNCPRG(NH_2)	$C_{46}H_{67}N_{15}O_{12}S_2$
HSA31−39	1115.47	LQQCPFEDH	$C_{48}H_{69}N_{13}O_{16}S_1$
somatostatin	1638.73	AGCKNFFWKTFTSC	$C_{76}H_{106}N_{18}O_{19}S_2$

Peptides were reduced by 0.13 M dithiothreitol in a 0.1 mL solution of sodium carbonate buffer at pH 8.2 at 56 °C for 1 h, and the reduced peptides were then purified using C18 ZipTip (Millipore; Billerica, MA, USA).

Mass Spectrometry. Unless noted otherwise, the reduced peptides were dissolved in a 50% methanol solution at 2 μM. For ETD experiments on metal−peptide complexes, the metal salt (100 μM final concentration) was added to the reduced peptide solution. The analyte solution was directly infused into an Orbitrap Velos Pro mass spectrometer (Thermo Fisher Scientific, Waltham, MA, USA) using a nanospray tip. The generated fragment ions were detected by either Orbitrap at a resolving power of 30 000 at m/z 400 or linear ion trap. For ETD experiments, 10^6 anions of fluoranthene were used for reaction, and the ion/ion reaction time was optimized in order to achieve a high signal-to-noise ratio for the ETD fragment ion peaks. The ion/ion reaction time exerted its effect on the precursor/product intensity ratio, but did not influence the $c^\bullet/c'$ and $z^\bullet/z'$ intensity ratio.

Notation. In the present study, Zubarev's unambiguous notation was adopted for peptide fragment ions.[19] According to this notation system, homolytic N−C_α bond cleavage yields the radical fragments $c^\bullet$ and $z^\bullet$, and addition of a hydrogen atom to $c^\bullet$ or $z^\bullet$ fragments produces the c' or z' fragment, respectively.

RESULTS AND DISCUSSION

ETD Mass Spectra of Cysteine-Containing Peptides with Different Precursor Ions. Somatostatin was used as a model to investigate the applicability of ETD MS to the cysteine-containing peptides. Triply protonated somatostatin, i.e., $[M+3H]^{3+}$ is mainly produced by ESI, since protonation preferentially occurs at the N-terminal amino group and the lysine residues at position 4 and 9. In the ETD mass spectrum of triply protonated precursor ions, b and y' ions were also observed as well as the typical c' and $z^\bullet$ ions (Figure 1a). The production of b and y' ions from peptide containing free cysteine residue is also reported in ECD experiment.[20] By contrast, the formation of b and y' ions was successfully suppressed by S-carbamidomethylation of the cysteine residue (data not shown). These results indicated that the thiol group of the cysteine residue contributes to b and y' ion generation by ETD. Since ECD/ETD preferentially produce c' and $z^\bullet$ fragments, peptide sequencing by ECD/ETD is generally carried out by interpreting mass differences between series of consecutive c' and $z^\bullet$ ions.[21] However, the presence of b and y' ions hampers the identification of sequence ions required for that purpose. In order to suppress b and y' ion formation, we used the group XII metal cations, which strongly bind to the thiol group, as a charge carrier. Complexation between group XII metal cation and cysteine containing peptide would lead to the deprotonation of thiol group. The ESI mass spectra of somatostatin with or without 100 μM group XII metal salts were compared, as shown in the right inset of Figure 1. The results indicate that the order of the metal−peptide complex yield is $Zn^{2+} \leq Cd^{2+} < Hg^{2+}$. In particular, the Hg^{2+}-aided method produced an intense signal of triply charged mercury-peptide complex, instead of $[M+3H]^{3+}$, probably due to strong interaction between Hg^{2+} and cysteine residues. Subsequently, we used the triply charged metal−peptide complexes, $[M+H+Zn]^{3+}$, $[M+H+Cd]^{3+}$, and $[M+H+Hg]^{3+}$ as precursor ions for ETD MS^2 measurement. As shown in the ETD mass spectra of triply charged zinc−, cadmium− and mercury−peptide complexes (Figure 1b−d), ETD of $[M+H+Zn]^{3+}$ and $[M+H+Cd]^{3+}$ mainly produced protonated and metal cationized c' and $z^\bullet$ fragments. In contrast, ETD of $[M+H+Hg]^{3+}$ gave an intense signal of the protonated radical cation, $[M + H]^{2+\bullet}$, instead of $c'/z^\bullet$ ions.

To date, the formation of the $c'/z^\bullet$ fragment pair has been believed to occur through electron transfer to a proton remote

dx.doi.org/10.1021/jp502818u | J. Phys. Chem. B 2014, 118, 12318−12325

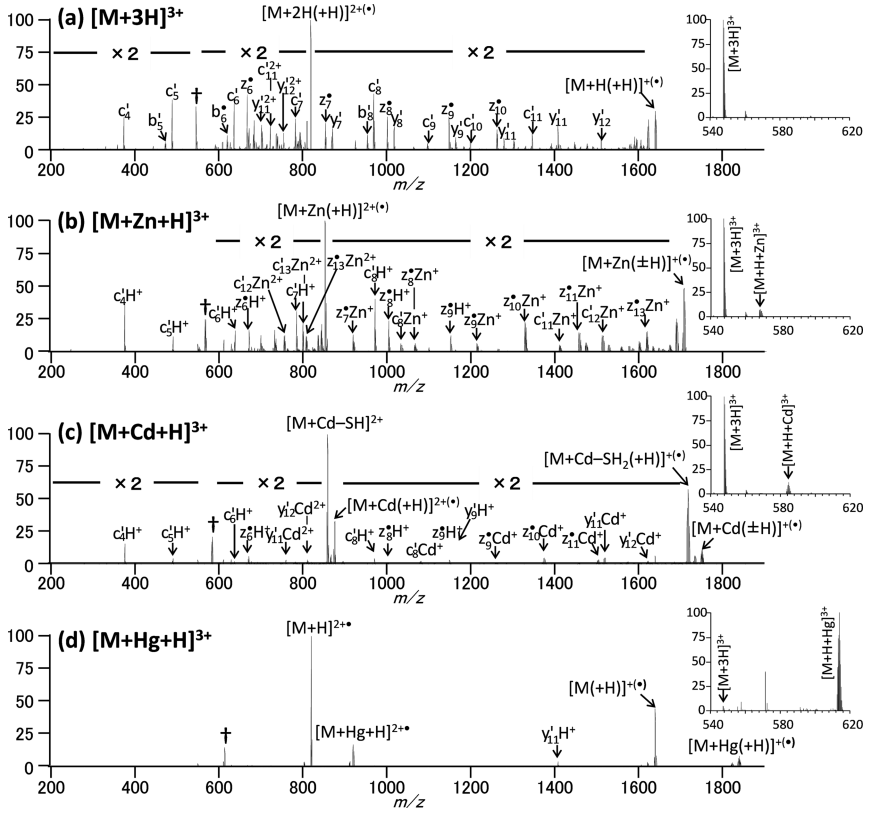

Figure 1. ETD spectra of triply charged somatostatin, (a) $[M+3H]^{3+}$, (b) $[M+H+Zn]^{3+}$, (c) $[M+H+Cd]^{3+}$, and (d) $[M+H+Hg]^{3+}$ detected by Orbitrap. Daggers indicate precursor ion signals. Inset panel: Enlargement ESI mass spectra for triply charged somatostatin.

from metal cation in the metal–peptide complex.[16] In contrast, the reduction of metal cations can occur in the metal–peptide complex, and the recombination energy of a metal cation and an electron is redistributed throughout the peptide to give *b*/*y* ions or neutral loss. These processes competitively occur in ECD/ETD of metal–peptide complexes. Flick et al. reported that the ECD phenomena of lanthanide–peptide complexes was dependent on the electrochemical properties of lanthanide cations in aqueous solution.[16] Consistent with their report, the Zn^{2+} bound to a peptide was barely reduced in ETD as compared with Cd^{2+} and Hg^{2+}, considering the order of their electron reduction potential in aqueous solution to be Zn^{2+} < Cd^{2+} < Hg^{2+}. As shown in Figure 1, ETD of $[M+H+Zn]^{3+}$ produced c' and $z^{\bullet}$ ions more abundantly than did those of $[M+H+Cd]^{3+}$ and $[M+H+Hg]^{3+}$, indicating that the decrease in the electron reduction potential of metal in the precursors increased the efficiency of proton/electron recombination and promoted the fragmentation yielding $c'/z^{\bullet}$ fragment pair. The $c'/z^{\bullet}$ ions were not observed in ETD of the mercury–peptide complex, because Hg^{2+} was reduced by ETD due to its electrochemical property. The differences in the fragment ions observed in the ETD spectra from various metal–peptide complexes would thus reflect the electrochemical properties of metal cations.

ETD of Zinc–Peptide Complexes. As shown in Figure 1b, ETD of zinc–peptide complex mainly produced c' and $z^{\bullet}$ fragments, which were formed through aminoketyl radical intermediate. ETD processes involving the zinc–peptide complex are summarized in Scheme 1a. Next, we focused on the ETD processes of the zinc–peptide complexes in more detail. In order to confirm the applicability of Zn^{2+}-aided ETD to sequencing of free cysteine-containing peptides, we analyzed

Scheme 1. Summary of Proposed Reactions in the ETD of (a) Zinc–, (b) Cadmium–, and (c) Mercury–Peptide Complexes

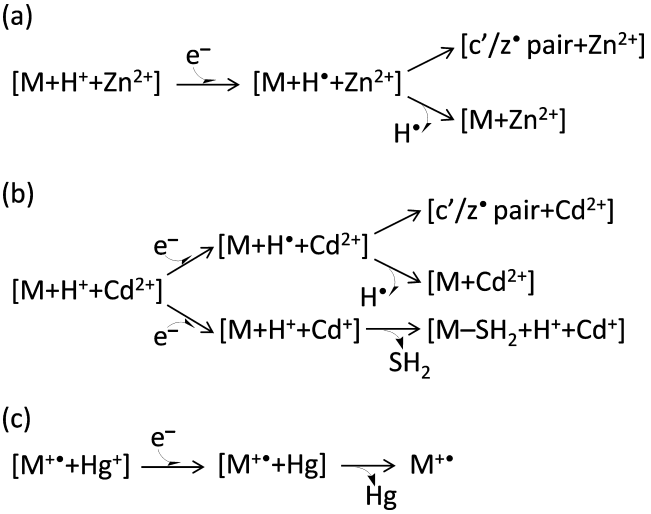

[Arg^8]-vasopressin. ESI dominantly produced doubly protonated [Arg^8]-vasopressin, since protonation preferentially occurs at N-terminal amino group and arginine residue at positon 8. However, double protonated peptide does not often provide enough information for peptide sequencing by ETD. Indeed, the ETD of $[M+2H]^{2+}$ yielded only three $z^{\bullet}$ fragments (Figure 2a). Although the triply protonated [Arg^8]-vasopressin, $[M+3H]^{3+}$ was absent, the Zn^{2+}-aided method produced a triply charged zinc-[Arg^8]-vasopressin complex, $[M+H+Zn]^{3+}$. Notably, five c' and five $z^{\bullet}$ fragments were observed in ETD

dx.doi.org/10.1021/jp502818u | J. Phys. Chem. B 2014, 118, 12318–12325

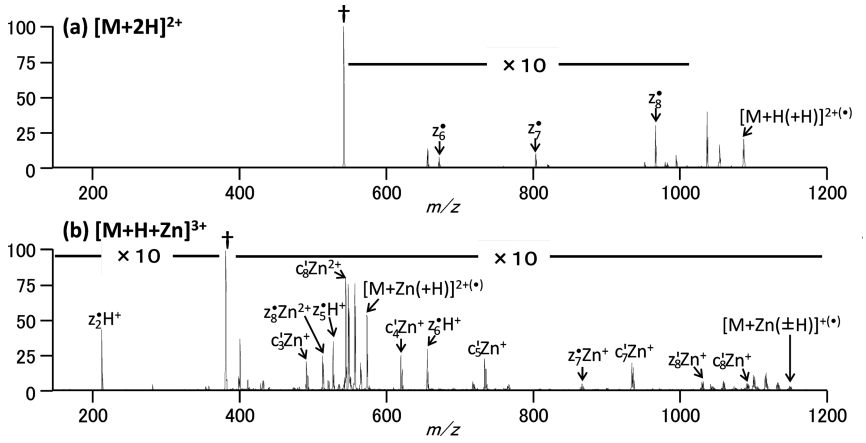

Figure 2. ETD mass spectra of [Arg^8]-vasopressin, (a) $[M+2H]^{2+}$ and (b) $[M+H+Zn]^{3+}$ detected by linear ion trap. Daggers indicate precursor ion signals.

mass spectrum of $[M+H+Zn]^{3+}$ (Figure 2b). Comparison of the ETD mass spectra of [Arg^8]-vasopressin with different precursors, $[M+H+Zn]^{3+}$ and $[M+2H]^{2+}$, indicates that the better sequence coverage was provided with higher charge state precursors. As demonstrated in the experiment, Zn^{2+}-aided ETD for the cysteine-containing peptide facilitated fragmentation by increasing the charge state of peptide ions and selective formation of c' and $z^{\bullet}$ ions from zinc−peptide complex would facilitate reading the peptide sequence, which is deduced by assignment of consecutive fragment ion series.

Notably, ETD of Zn^{2+}−peptide complexes generates abundant signal of the $c^{\bullet}$ and z' fragments. These product are often observed in ECD mass spectra. The abundance of $c^{\bullet}$ and z' fragments in ECD is rationalized on the basis of the long lifetime of the c'-$z^{\bullet}$ complex, allowing interfragment hydrogen migration.[10,12] For considering the difference between ECD and ETD, the electron transfer from fluoranthene anion to peptide ion is less exothermic than electron capture process of peptide ion. Since ETD is performed in ion trap, the generated aminoketyl radical takes place collisional cooling, reducing their internal energy. The experimental difference in ECD and ETD would affect the abundance of $c^{\bullet}$ and z' fragments. Nevertheless, increasing the internal energy of the precursor by vibrational activation during ECD and ETD can suppress the formation of $c^{\bullet}$ and z' fragments.[22,23] Despite these differences in experimental conditions, it is suggested that ECD and ETD involve the formation of $c'-z^{\bullet}$ complex, which eventually leads to the $c^{\bullet}$ and z' fragments by interfragment hydrogen migration.

We recently demonstrated that the presence of a metal cation in the precursor for ETD increases the lifetime of the $c'-z^{\bullet}$ fragment complex, and the degree of hydrogen migration was dependent on the location of the metal cation in the radical intermediate.[10] To estimate the efficiency of the interfragment hydrogen migration in ETD, we used a modified method according to the procedure proposed by Nishikaze et al.[24]

$$H_{tn} = \frac{I[z'_n]}{I[z_n^{\bullet}] + I[z'_n]} \times 100, \qquad \frac{I[c_n^{\bullet}]}{I[c_n^{\bullet}] + I[c'_n]} \times 100$$

where I is the intensity of fragment ions. In the present study, the abundances of c' and z' ions were compensated using theoretical isotopic contributions of $c^{\bullet}$ and $z^{\bullet}$ ions, respectively, and the intensity of fragment ions, I, was calculated from the signal intensity appeared at their monoisotopic mass. To obtain well-reproducible results, 20 μM of analyte solution with 500 μM of $ZnCl_2$ was used this experiments. The H_{tn} values were determined by averaging three ETD mass spectra. The H_{tn} values obtained from the zinc−[Arg^8]-vasopressin complex are summarized in Scheme 2a. The high H_{tn} values for the

Scheme 2. Observed Fragment Ions in ETD Mass Spectra of Peptides with Different Precursors and Their H_{tn} Values

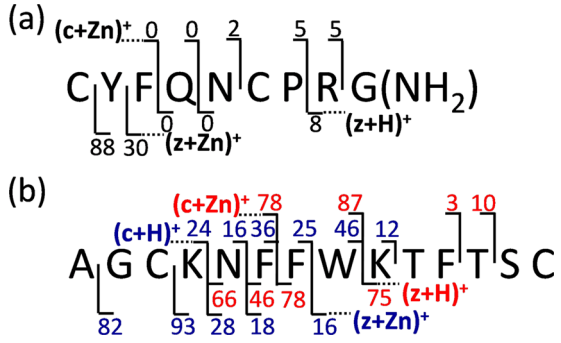

cleavages at the Cys1−Tyr2 and Tyr2−Phe3 bonds were derived from interfragment hydrogen migration, suggesting the $c_1'/z_8^{\bullet}$ and $c_2'/z_7^{\bullet}$ complexes to be a long-lived radical intermediate held together through zinc−peptide binding. Since the charge reduction of precursor ions, which is the initial step of ETD, caused substantial conformational rearrangement,[10] the H_{tn} value would be dependent on the location of Zn^{2+} in the "proton-removed" precursor. Therefore, we focused on the $[M+Zn]^{2+}$ conformation of [Arg^8]-vasopressin, in order to understand the role of high H_{tn} values in the cleavages at the Cys1−Tyr2 and Tyr2−Phe3 bonds in the ETD mass spectrum of $[M+H+Zn]^{3+}$. According to an ab initio calculation for the Zn^{2+}−cysteine complex, Zn^{2+} is bound to a sulfur atom of cysteine to form a zwitterion in which the thiol group is deprotonated and a proton is located at the amino group. This suggested that, in the zinc−[Arg^8]-vasopressin complex $[M+Zn]^{2+}$ the cysteine residue is deprotonated, and a proton is located on the arginine residue at position 8, the most efficient protonation site of the peptide. [Arg^8]-vasopressin contains two cysteine residues at positions 1 and 6, but the residue at position 6 could not interact with Zn^{2+} due to Coulomb repulsion between Zn^{2+} and the protonated arginine at position 8. Consequently, Zn^{2+} would be

dx.doi.org/10.1021/jp502818u | J. Phys. Chem. B 2014, 118, 12318−12325

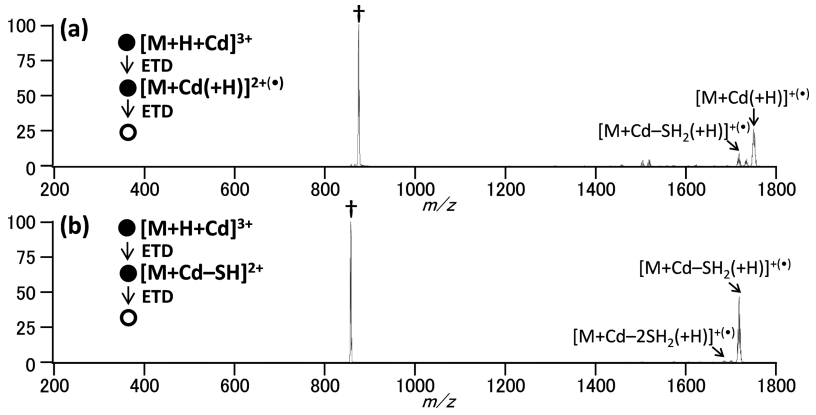

Figure 3. ETD mass spectra of somatostatin, (a) $[M+Cd(+H)]^{2+(\bullet)}$ and (b) $[M+Cd-SH]^{2+}$ generated from $[M+H+Cd]^{3+}$ by ETD detected by linear ion trap. Daggers indicate precursor ion signals.

coordinated with the N-terminal region of [Arg^8]-vasopressin. The formation of $[z_7'-H+Zn]^+$ and $[z_8'-H+Zn]^+$ from ETD of the $[M+H+Zn]^{3+}$ indicated that interfragment hydrogen migration occurred in the region encompassing positions 1 to 3. The Zn^{2+} was located in the N-terminal side of the intermediate, and the H_{tn} value could be reconciled with conformation of the "proton-removed" precursor.

Next, we focused on the interfragment hydrogen migration that occurs during the ETD processes involving the zinc-somatostatin complex $[M+H+Zn]^{3+}$. The ETD mass spectrum showed four different types of fragment ions, $[c_n'/c_n^{\bullet}+H]^+$, $[c_n'/c_n^{\bullet}-H+Zn]^+$, $[z_n^{\bullet}/z_n'+H]^+$, and $[z_n^{\bullet}/z_n'-H+Zn]^+$, which made interpretation of the H_{tn} values difficult. Notably, the degree of interfragment hydrogen migration differs between protonated fragments and the corresponding zinc adducted fragments, indicating that the conformations of intermediates yielding these fragment ions differed from each other. The proton in $[M+H+Zn]^{3+}$ was reduced via ion/ion reaction, and the resulting doubly charged intermediate would have produced either the $[c_n'+H]^+/[z_{(m-n)}^{\bullet}-H+Zn]^+$ ion pair, or the $[c_n'-H+Zn]^+/[z_{(m-n)}^{\bullet}+H]^+$ ion pair (m indicates number of amino acid residues in peptide). It was suggested that the conformation of the intermediate generating the $[c_n'+H]^+/[z_{(m-n)}^{\bullet}-H+Zn]^+$ ion pair differed from that yielding the $[c_n'-H+Zn]^+/[z_{(m-n)}^{\bullet}+H]^+$ ion pair. The H_{tn} values of the $[c_n'+H]^+/[z_{(m-n)}^{\bullet}-H+Zn]^+$ (blue number) and $[c_n'-H+Zn]^+/[z_{(m-n)}^{\bullet}+H]^+$ (red number) ion pairs are summarized in Scheme 2b. The H_{tn} values of complementary $[c_n'+H]^+$ and $[z_{(m-n)}^{\bullet}-H+Zn]^+$ were similar, indicating hydrogen migration to occur between the mutually complementary pair of $[c_n'+H]^+$ and $[z_{(m-n)}^{\bullet}-H+Zn]^+$. The H_{tn} values in the region encompassing 1 to 3 were high, and thus revealed the location of Zn^{2+} in the intermediate yielding the $[c_n'+H]^+/[z_{(m-n)}^{\bullet}-H+Zn]^+$ ion pair. In contrast, the interfragment hydrogen migration occurred in the region encompassing 4 to 8 during formation of the $[c_n'-H+Zn]^+/[z_{(m-n)}^{\bullet}+H]^+$ ion pair. Since the protonated $z^{\bullet}$ fragment was observed to be derived from $z_5^{\bullet}$, a proton was localized on the lysine residue at position 9 in the intermediate. As a result, Zn^{2+} was coordinated with the N-terminal region of the intermediate yielding the $[c_n'-H+Zn]^+/[z_{(m-n)}^{\bullet}+H]^+$ ion pair.

ETD of Cadmium–Peptide Complexes. The cadmium-peptide complex generated c' and $z^{\bullet}$ fragments by ETD, as in the case of the zinc–peptide complex (Figure 1c). However, the yield of c' and $z^{\bullet}$ ions in the ETD spectrum of the cadmium–peptide complex was lower than that of the corresponding zinc–peptide complex. The metal–peptide complex undergoes either hydrogen radical production or metal cation reduction by ECD/ETD, according to the electrochemical properties of metal cations in the precursor. The presence of Cd^{2+} instead of Zn^{2+} in the precursor would reduce the yield of the aminoketyl radical intermediate, due to the higher electron reduction potential of Cd^{2+} than Zn^{2+}. By contrast, ETD of $[M+H+Cd]^{3+}$ produced an intense signal of $[M+Cd-SH]^{2+}$ (Figure 1c). The $[M+Cd-SH]^{2+}$ was formed by SH_2 loss from the precursor, which was not formed via the aminoketyl radical intermediate. Since the Cd^{2+} bound to a peptide would easily be reduced as compared with Zn^{2+} in ETD, the SH_2 loss from the cadmium–peptide complex was probably mediated by recombination energy between Cd^{2+} and an electron. Notably, ETD of $[M+H+Cd]^{3+}$ yielded singly charge species, $[M+Cd(\pm H)]^+$ and $[M+Cd-SH_2]^+$, but not $[M+Cd-2SH_2]^+$, despite the precursor having two cysteine residues. To investigate the metal reduction process in detail, we scrutinized the ETD MS^3 spectra of $[M+Cd(+H)]^{2+(\bullet)}$ and $[M+Cd-SH]^{2+}$ (Figure 3). ETD induced the charge reduction of $[M+Cd(+H)]^{2+(\bullet)}$ with or without SH_2 loss, generating $[M+Cd(+H)]^{2+(\bullet)}$ or $[M+Cd-SH(+H)]^{2+}$ (Figure 3a). In contrast, ETD of $[M+Cd-SH]^{2+}$ mainly produced $[M+Cd-SH_2(+H)]^{2+}$, while $[M+Cd-2SH_2]^+$ was barely generated (Figure 3b). These results indicated that the transfer of two electrons to $[M+H+Cd]^{2+}$ led to loss of one SH_2 and were attributable to the different ionization energies of Cd^+ and Cd^{2+}. The Cd^+ in the complex was barely reduced as compared with Cd^{2+} by ETD, since the ionization energy for Cd (8.99 eV) is much lower than that for Cd^+ (16.91 eV). ETD of cadmium–peptide complexes generated an intermediate, $[M+H+Cd]^{2+}$, containing monovalent cadmium (Cd^+) due to reduction of Cd^{2+}, eventually leading to loss of SH_2, giving $[M+Cd-SH]^{2+}$. However, the resulting Cd^+ in the complex did not undergo further reduction due to its low electron reduction potential, and thus the further SH_2 loss to form $[M+Cd-2SH_2]^+$ was not a dominant process.

To obtain direct evidence for the presence of Cd^+ in $[M+Cd-SH]^{2+}$, we performed MS^3 analysis with CID, but interpretation of the CID spectrum of $[M+Cd-SH]^{2+}$ for somatostatin was difficult due to the presence of two cysteine residues (data not shown). Instead, a synthetic peptide corresponding to residues 31–39 of human serum albumin (i.e., the aforementioned HSA31–39) containing one cysteine

dx.doi.org/10.1021/jp502818u | J. Phys. Chem. B 2014, 118, 12318–12325

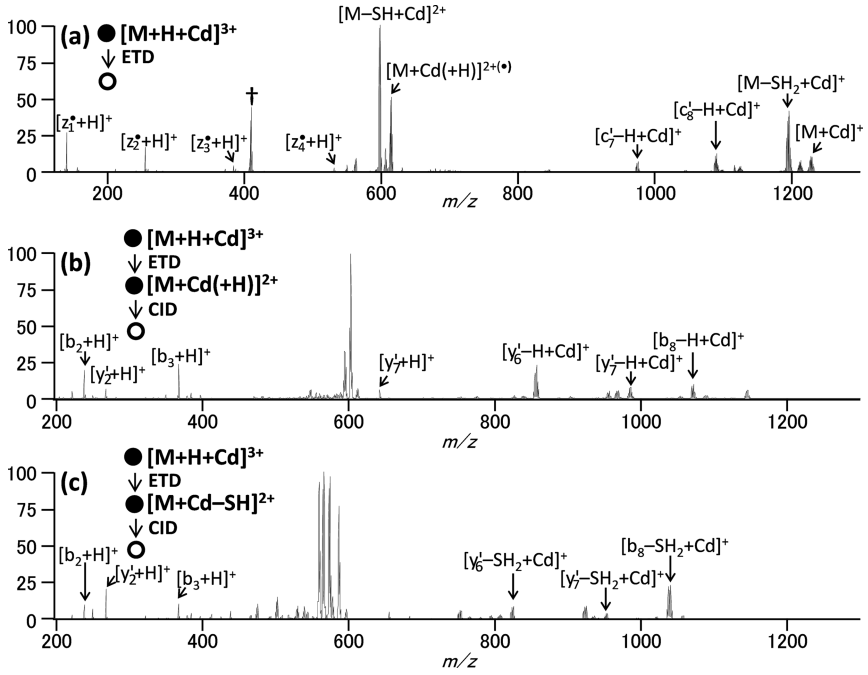

Figure 4. (a) MS^2, ETD mass spectrum of HSA31−39 detected by Orbitrap. MS^3, CID mass spectra of (b) $[M+Cd(+H)]^{2+(\bullet)}$ and (c) $[M+Cd-SH]^{2+}$, shown in panel a, detected by linear ion trap. Daggers indicate precursor ion signals.

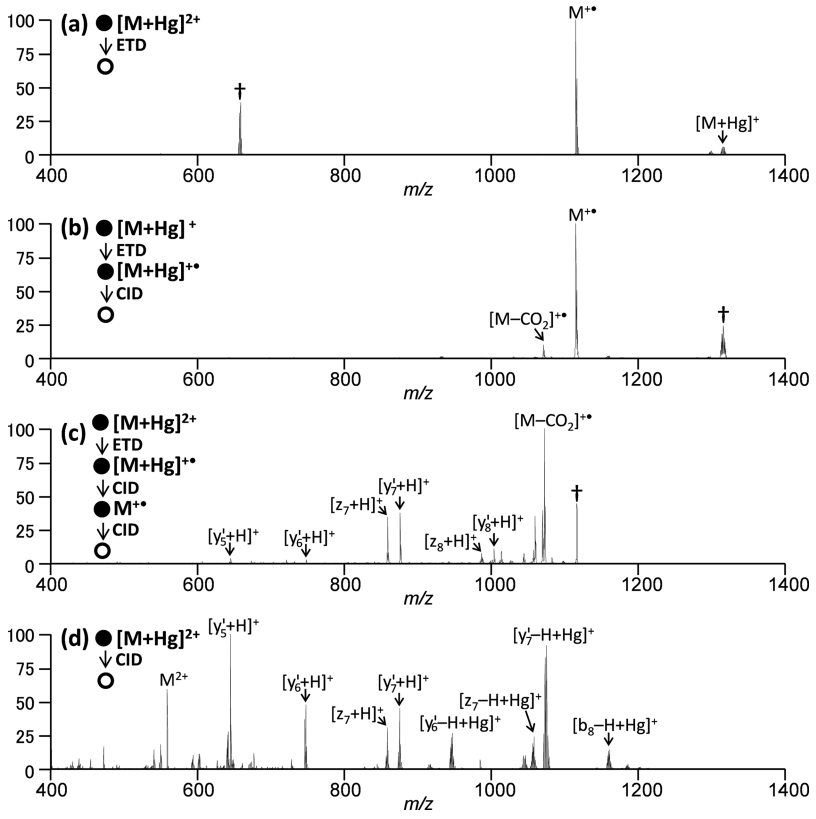

Figure 5. (a) MS^2, ETD mass spectrum of HSA31−39, $[M+Hg]^{2+}$ detected by Orbitrap. (b) MS^3, CID mass spectrum of $[M+Hg]^{+\bullet}$ shown in panel a, detected by linear ion trap. (c) MS^4, CID mass spectrum of $M^{+\bullet}$ shown in panel b, detected by linear ion trap. (d) CID mass spectra of $[M+Hg]^{2+}$ detected by Orbitrap. Daggers indicate precursor ion signals.

residue was analyzed. ETD of the triply charged Cd^{2+}-HSA31−39 complex $[M+H+Cd]^{3+}$ produced $c'/z^{\bullet}$ fragments, $[M+Cd(+H)]^{2+(\bullet)}$ and $[M+Cd-SH]^{2+}$, as in the case of somatostatin (Figure 4a). The CID mass spectra of the ETD products, $[M+Cd(+H)]^{2+(\bullet)}$ and $[M+Cd-SH]^{2+}$, showing both metalated and protonated fragments, are presented for comparison in Figure 4b,c. The metalated fragment from CID of $[M+Cd(+H)]^{2+(\bullet)}$ was observed as a zwitterion form,

dx.doi.org/10.1021/jp502818u | J. Phys. Chem. B 2014, 118, 12318−12325

$[y'_n-H+Cd]^+$, containing divalent cadmium, Cd^{2+}. In contrast, CID of $[M+Cd-SH]^{2+}$ generated singly charged cadmium adducts fragments, indicating cadmium in the precursor to be the monovalent form, Cd^+. Therefore, Cd^{2+} in the complex was reduced by ETD and the recombination energy of Cd^{2+} and the electron was converted to the internal energy of the complex with subsequent SH_2 loss. ETD processes of the cadmium−peptide complex are summarized in Scheme 1b.

ECD of Cd^{2+}-tryptophan containing peptide complexes has been demonstrated to generate the peptide radical cation by reduction of Cd^{2+}.[15] In contrast, no peptide radical cation was observed in ETD mass spectra of cadmium−cysteine containing peptide complexes. These differences are probably due to the different ionization energies of tryptophan and cysteine. Among amino acids, tryptophan has the lowest ionization energy.[25] In fact, the conversion of tryptophan into valine strongly suppresses peptide radical formation by ECD of the cadmium−peptide complex.[15] The recombination energy between an electron and Cd^{2+} in the complex would be enough for ionization of the tryptophan residue, but not cysteine and valine residues.

ETD of Mercury−Peptide Complexes. As shown in Figure 1d, a peptide radical cation was formed by ETD of the mercury−somatostatin complex. The same results were obtained with two cysteine-containing peptides, [Arg[8]]-vasopressin and HSA31−39. The complexes, $[M+H+Hg]^{3+}$ and $[M+Hg]^{2+}$, preferentially yielded $[M+H]^{2+\bullet}$ and $M^{+\bullet}$, respectively. To address the mechanism of radical cation formation in ETD of mercury−peptide complexes in more detail, we performed MS^n analysis of mercury-HSA31−39 complex. ETD of the triply charged mercury-HSA31−39 complex $[M+Hg]^{2+}$ produced doubly charged product ions, $M^{+\bullet}$ and $[M+Hg]^{+\bullet}$, via an electron transfer event (Figure 5a). Subsequently, $[M+Hg]^{+\bullet}$ was analyzed by CID (Figure 5b). Interestingly, an intense signal of the radical cation $M^{+\bullet}$, which was formed by mercury atom loss, was observed in the product ion mass spectrum (Figure 5c). This finding suggested Hg^{2+} in the mercury−peptide complex to be reduced by an ion/ion reaction, giving off the intermediate radical $[M+Hg]^{+\bullet}$ which carries a charge on Hg^+. CID of $[M+Hg]^{+\bullet}$ might have induced the charge transfer between Hg^+ and the peptide, giving $M^{+\bullet}$ and a mercury atom. However, an intense $M^{+\bullet}$ signal was observed in the ETD mass spectrum (Figure 5a). This result indicated that an electron transfer to the mercury−peptide complex led to the efficient loss of a mercury atom, despite mercury being a divalent cation. In addition, CID of the radical cation $M^{+\bullet}$ was performed. The CID spectrum of $M^{+\bullet}$ (MS^4, $[M+Hg]^{2+} \rightarrow [M+Hg]^{+\bullet} \rightarrow M^{+\bullet}$, Figure 5c) showed a pattern quite similar to that of the corresponding ions directly formed by ETD (MS^3, $[M+Hg]^{2+} \rightarrow M^{+\bullet}$, data not shown), indicating these products to have the same chemical state. Therefore, the $[M+Hg]^{+\bullet}$ observed in the ETD spectrum of $[M+Hg]^{2+}$ was suggested to be an intermediate of radical cation, $M^{+\bullet}$.

To understand the peptide radical cation formation process mediated by reduction of Hg^{2+}, we considered the structure of the mercury−peptide complex. According to ab initio calculation of the interaction between Hg^{2+} and cysteine, Hg^{2+} is coordinated with the thiolate group ($-S^-$) to form a complex.[26] Notably, the natural charge of mercury in the complex with the lowest energy conformation is only +0.79e.[26] An electron transfer to mercury in the mercury−cysteine complex would give a neutral mercury atom and a cysteine radical cation. In addition, we performed CID of the mercury−HSA31−39 complex $[M+Hg]^{2+}$, which produced a doubly charged peptide, M^{2+}, via mercury atom loss (Figure 5d). Since the formation of M^{2+} involved heterolytic cleavage of the coordinate bond between cysteine and mercury ($-S^- \rightarrow Hg^{2+}$), the result supported the presence of a coordinate bond between the cysteine residue and Hg^{2+}. Therefore, this process reasonably explains the mechanism by which the peptide radical cation is formed via transfer of an electron to the mercury−peptide complex. ETD processes involving the mercury−peptide complex are summarized in Scheme 1c.

The chemical properties of peptide radical cation, $M^{+\bullet}$ have been investigated through collision-induced dissociation (CID) of Cu^{2+}-ligand−peptide complexes.[27] Collisional activation of Cu^{2+}-ligand−peptide complexes induces an electron abstraction from peptide moiety, generating $M^{+\bullet}$. Peptides containing an aromatic residue formed abundant peptide radical cation through CID of Cu^{2+}-ligand−peptide complexes. Tryptophan and tyrosine residues are easily cationized due to their low ionization energy[25] and produce abundant radical cation containing the charge and radical sites at aromatic side chain.[28] In the other case, peptide radical cation took a protonated hydrogen-deficient radical form in which the α-carbon was radical center and that a proton was present elsewhere in the peptide.[27] In contrast, the presented method, Hg^{2+}-aided ETD gave intense $M^{+\bullet}$ signal of HSA31−39, which does not contain any tryptophan and tyrosine residues. Hg^{2+} bind to the thiol group of cysteine residues in peptides and the yield of Hg^{2+}−peptide complex was strongly decreased by S-carbamidomethylation of the cysteine residue. Therefore, Hg^{2+}-aided ETD is suitable method for investigation of peptide radical cation containing free cysteine residue.

Additionally, Hg^{2+}-aided CID produced doubly charged peptide, M^{2+} and can open the possibility to investigate chemical properties of M^{2+} in the gas phase. However, M^{2+} was not consistently observed in CID mass spectra of mercury−peptide complexes and the formation efficiency of M^{2+} is dependent on the amino acid sequence of the peptide. For example, the CID of mercury−[Arg[8]]-vasopressin generated nonmetalated doubly charged products with neutral losses, giving $[M-NH_3]^{2+}$ and $[M-SH_2]^{2+}$ (data not shown). By contrast, the mercury−somatostatin complex generated no doubly charged fragments (data not shown). The effects of amino acid sequences on the formation of M^{2+} require further investigation. The Hg^{2+}-aided CID holds promise for studying the gas-phase chemistry of doubly charged peptides, M^{2+}, although the formation mechanism from mercury−peptide complexes has yet to be elucidated.

CONCLUSION

The fragmentation efficiency and peptide sequence coverage by ETD is generally enhanced by increasing the charge state of precursor peptide ions. The use of a suitable metal ion in ESI can increase the charge state of peptide ions. Since the group XII metal ions strongly bind to the thiol group, we used these ions to increase the charge state of free-cysteine containing peptide formed by ESI and investigated ETD processes of the group XII metal−peptide complexes by multistage tandem mass spectrometry. ETD processes of complex formation were influenced by the electrochemical properties of the metal cations. The Zn^{2+} in the zinc−peptide complex was barely reduced by ETD and $c'/z^{\bullet}$ fragment pairs were preferentially formed. The Zn^{2+}-aided method has the potential to increase the charge state of cysteine-containing peptides, improving the

sequence coverage of these peptides. By contrast, the Cd^{2+} in the complex was easily reduced by ETD as compared with Zn^{2+} and the metal cation and proton reductions occurred competitively in ETD of the cadmium−peptide complex. The $c'/z^{\bullet}$ fragment pair was barely formed by ETD of mercury−peptide complex due to the high reduction potential of Hg^{2+}. Alternatively, a peptide radical cation and neutral mercury were produced by ETD. Thus, while Hg^{2+}-aided ETD and CID may not be useful for proteomic studies, it is anticipated to facilitate understanding of gas-phase peptide radical chemistry.

AUTHOR INFORMATION

Corresponding Author

*Address: 6-2-3 Furuedai, Suita, Osaka, 565-0874, Japan. E-mail: daiki.asakawa@riken.jp. Phone: +81-661550448.

Present Address

[†]RIKEN Quantitative Biology Center, 6-2-3 Furuedai, Suita, Osaka, 565−0874, Japan.

Notes

The authors declare no competing financial interest.

ACKNOWLEDGMENTS

The authors thank Dr. Hajime Mizuno and Dr. Tsutomu Masujima (RIKEN, Qbic) for kindly providing access to the Thermo-Fisher Orbitrap Velos Pro instrument. Daiki Asakawa gratefully acknowledges a research fellowship from the Japan Society for the Promotion of Science for Young Scientists (23-10272).

REFERENCES

(1) Zubarev, R. A.; Kelleher, N. L.; McLafferty, F. W. Electron Capture Dissociation of Multiply Charged Protein Cations. A Nonergodic Process. *J. Am. Chem. Soc.* **1998**, *120*, 3265−3266.

(2) Syka, J. E.; Coon, J. J.; Schroeder, M. J.; Shabanowitz, J.; Hunt, D. F. Peptide and Protein Sequence Analysis by Electron Transfer Dissociation Mass Spectrometry. *Proc. Natl. Acad. Sci. U. S. A.* **2004**, *101*, 9528−9533.

(3) Tureček, F.; Julian, R. R. Peptide Radicals and Cation Radicals in the Gas Phase. *Chem. Rev.* **2013**, *113*, 6691−6733.

(4) Frese, C. K.; Altelaar, A. F.; Hennrich, M. L.; Nolting, D.; Zeller, M.; Griep-Raming, J.; Heck, A. J.; Mohammed, S. Improved Peptide Identification by Targeted Fragmentation Using CID, HCD and ETD on an LTQ-Orbitrap Velos. *J. Proteome Res.* **2011**, *10*, 2377−2388.

(5) Rožman, M.; Gaskell, S. J. Charge State Dependent Top-Down Characterisation Using Electron Transfer Dissociation. *Rapid Commun. Mass Spectrom.* **2012**, *26*, 282−286.

(6) Ueberheide, B. M.; Fenyo, D.; Alewood, P. F.; Chait, B. T. Rapid Sensitive Analysis of Cysteine Rich Peptide Venom Components. *Proc. Natl. Acad. Sci. U. S. A.* **2009**, *106*, 6910−6915.

(7) Vasicek, L.; Brodbelt, J. S. Enhanced Electron Transfer Dissociation through Fixed Charge Derivatization of Cysteines. *Anal. Chem.* **2009**, *81*, 7876−7884.

(8) Ko, B. J.; Brodbelt, J. S. Enhanced Electron Transfer Dissociation of Peptides Modified at C-Terminus with Fixed Charges. *J. Am. Soc. Mass Spectrom.* **2012**, *23*, 1991−2000.

(9) Frey, B. L.; Ladror, D. T.; Sondalle, S. B.; Krusemark, C. J.; Jue, A. L.; Coon, J. J.; Smith, L. M. Chemical Derivatization of Peptide Carboxyl Groups for Highly Efficient Electron Transfer Dissociation. *J. Am. Soc. Mass Spectrom.* **2013**, *24*, 1710−1721.

(10) Asakawa, D.; Takeuchi, T.; Yamashita, A.; Wada, Y. Influence of Metal−Peptide Complexation on Fragmentation and Inter-Fragment Hydrogen Migration in Electron Transfer Dissociation. *J. Am. Soc. Mass Spectrom.* **2014**, *25*, 1029−1039.

(11) Iavarone, A. T.; Paech, K.; Williams, E. R. Effects of Charge State and Cationizing Agent on the Electron Capture Dissociation of a Peptide. *Anal. Chem.* **2004**, *76*, 2231−2238.

(12) Fung, Y. M.; Liu, H.; Chan, T. W. Electron Capture Dissociation of Peptides Metalated with Alkaline-Earth Metal Ions. *J. Am. Soc. Mass Spectrom.* **2006**, *17*, 757−771.

(13) Liu, H.; Håkansson, K. Divalent Metal Ion−Peptide Interactions Probed by Electron Capture Dissociation of Trications. *J. Am. Soc. Mass Spectrom.* **2006**, *17*, 1731−1741.

(14) Chen, X.; Fung, Y. M.; Chan, W. Y.; Wong, P. S.; Yeung, H. S.; Chan, T. W. Transition Metal Ions: Charge Carriers that Mediate the Electron Capture Dissociation Pathways of Peptides. *J. Am. Soc. Mass Spectrom.* **2011**, *22*, 2232−2245.

(15) Chen, X.; Chan, W. Y.; Wong, P. S.; Yeung, H. S.; Chan, T. W. Formation of Peptide Radical Cations ($M^{+}\bullet$) in Electron Capture Dissociation of Peptides Adducted with Group IIB Metal Ions. *J. Am. Soc. Mass Spectrom.* **2011**, *22*, 233−244.

(16) Flick, T. G.; Donald, W. A.; Williams, E. R. Electron Capture Dissociation of Trivalent Metal Ion-Peptide Complexes. *J. Am. Soc. Mass Spectrom.* **2013**, *24*, 193−201.

(17) O'Connor, P. B.; Lin, C.; Cournoyer, J. J.; Pittman, J. L.; Belyayev, M.; Budnik, B. A. Long-Lived Electron Capture Dissociation Product Ions Experience Radical Migration via Hydrogen Abstraction. *J. Am. Soc. Mass Spectrom.* **2006**, *17*, 576−585.

(18) Kohtani, M.; Jarrold, M. F.; Wee, S.; O'Hair, R. A. Metal Ion Interactions with Polyalanine Peptide. *J. Phys. Chem. B* **2004**, *108*, 6093−6097.

(19) Zubarev, R. A. Reactions of Polypeptide Ions with Electrons in the Gas Phase. *Mass Spectrom. Rev.* **2003**, *22*, 57−77.

(20) Nicolardi, S.; Giera, M.; Kooijman, P.; Kraj, A.; Chervet, J. P.; Deelder, A. M.; van der Burgt, Y. E. On-Line Electrochemical Reduction of Disulfide Bonds: Improved FTICR-CID and -ETD Coverage of Oxytocin and Hepcidin. *J. Am. Soc. Mass Spectrom.* **2013**, *24*, 1980−1987.

(21) Zhurov, K. O.; Fornelli, L.; Wodrich, M. D.; Laskay, U. A.; Tsybin, Y. O. Principles of Electron Capture and Transfer Dissociation Mass Spectrometry Applied to Peptide and Protein Structure Analysis. *Chem. Soc. Rev.* **2013**, *42*, 5014−5030.

(22) Tsybin, Y. O.; He, H.; Emmett, M. R.; Hendrickson, C. L.; Marshall, A. G. Ion Activation in Electron Capture Dissociation to Distinguish between N-Terminal and C-Terminal Product Ions. *Anal. Chem.* **2007**, *79*, 7596−7602.

(23) Ledvina, A. R.; McAlister, G. C.; Gardner, M. W.; Smith, S. I.; Madsen, J. A.; Schwartz, J. C.; Stafford, G. C., Jr.; Syka, J. E.; Brodbelt, J. S.; Coon, J. J. Infrared Photoactivation Reduces Peptide Folding and Hydrogen-Atom Migration Following ETD Tandem Mass Spectrometry. *Angew. Chem., Int. Ed.* **2009**, *48*, 8526−8528.

(24) Nishikaze, T.; Takayama, M. Influence of Charge State and Amino Acid Composition on Hydrogen Transfer in Electron Capture Dissociation of Peptides. *J. Am. Soc. Mass Spectrom.* **2010**, *21*, 1979−1988.

(25) Close, D. M. Calculated Vertical Ionization Energies of the Common α-Amino Acids in the Gas Phase and in Solution. *J. Phys. Chem. A* **2011**, *115*, 2900−2912.

(26) Mori, S.; Endoh, T.; Yaguchi, Y.; Shimizu, Y.; Kishi, T.; Yanai, T. K. Quantum Chemical Studies on the Role of Water Microsolvation in Interactions Between Group 12 Metal Species (Hg^{2+}, Cd^{2+}, and Zn^{2+}) and Neutral and Deprotonated Cysteines. *Theor. Chem. Acc.* **2011**, *130*, 279−297.

(27) Hopkinson, A. C. Radical Cations of Amino Acids and Peptides: Structures and Stabilities. *Mass Spectrom. Rev.* **2009**, *28*, 655−671.

(28) Bagheri-Majdi, E.; Ke, Y.; Orlova, G.; Chu, I. K.; Hopkinson, A. C.; Siu, K. W. M. Copper-Mediated Peptide Radical Ions in the Gas Phase. *J. Phys. Chem. B* **2004**, *108*, 11170−11181.